

HIGH CURRENT GAIN HETEROJUNCTION BIPOLAR PHOTOTRANSISTOR FOR MONOLITHIC INTEGRATED PHOTORECEIVER

HAILA WANG and DAVID ANKRI

Centre national d'études des telecommunications laboratoire de Bagneux, 196, Avenue Henri Ravera,
92220 Bagneux, France

(Received 8 April 1986; in revised form 20 July 1986)

Abstract—The first monolithic photoreceiver integrating an HPT, two HBT's on a GaAs chip has been designed, fabricated and tested. A sensitivity of -30 dBm for 140 Mbit/s transmission rate was inferred from signal to noise ratio measurement. Taking into account the specific characteristics of high current gain-high speed heterojunction phototransistor, the receiver sensitivity has been analysed. For high current gain HPT's, the base layer is very thin and in this case, the early effect and the thermal noise of the base access resistance have to be taken into account. This leads to a trade-off between the base resistance and the current gain. Compared to PIN-FET receivers, the range of interest for HPT, from the point of view of sensitivity is located above a few hundreds Mbit/s, but for a monolithic photoreceiver implemented with HPT and heterojunction bipolar transistors (HBT's) and advantages of monolithic integration leads to an extension of the application range.

NOTATION

C_c	base-collector junction capacitance
C_d	emitter-base diffusion capacitance
C_{ej}	emitter-base junction capacitance
f	frequency
f_T	cutoff frequency
H_{ph}	Fourier transform of the received pulse shape
H_{out}	Fourier transform of the output pulse shape
h	Planck's constant
i_A	total equivalent noise current density
I_b	recombination current in the base
I_c	collector current
$I_{c,opt}$	optimum collector current
I_r	recombination current in the base-emitter space-charge region
m	diode ideality factor of total base current
n	diode ideality factor of collector current
P_m	minimum detectable power
q	electronic charge
R_b	base access resistance
R_e	U_T/I_c
R_f	bias and feedback resistance
T	bit periode
V_{be}	base-emitter applied voltage
U_T	thermal voltage
Z	noise parameter
β	d.c. current gain
η	detector Quantum efficiency
Ω	optical frequency.

1. INTRODUCTION

The advent of optical transmissions has created a large demand of high sensitivity photoreceivers for a wide variety of systems. Many efforts have been made in order to optimize signal to noise ratio. The monolithic integration of different configurations of preamplifier circuit associating different photodetectors has been studied for reducing the parasitic noise[1–3], and the comparison between different photodetector-preamplifiers has been carried out to

design the most suitable detector-preamplifier for each bit-rate and error-rate requirement[4–6]. Compared to HPT and PIN-FET, the APD has many disadvantages for practical systems applications, especially for local area networks because a complex additional circuit is required to maintain the APD at optimum gain over full operating temperature range. HPT and PIN-FET are more comparable. In addition to their high sensitivity at high bit-rates, HPT's have a structure similar to HBT's which is very useful for monolithic integration, and as for all bipolar devices, this can be obtained with a large bandwidth and a high temperature stability.

In this paper, the HPT receiver sensitivity is analyzed taking into account the specific characteristics of high gain-high speed heterojunction phototransistors with respect to the fabrication technology for diffused and non-diffused transistors. The design of a monolithic integrated transimpedance photoreceiver using an HPT and HBT's is discussed. The experimental results on a first monolithic photoreceiver are compared with the predicted results. Microwave characterizations of HPT and HBT have been done using S-parameter measurements. Finally, the electrical equivalent circuits of HBT and HPT lead to the main physical parameters which control the sensitivity performance.

2. HPT ANALYSIS AND COMPARISON OF TWO HPT's STRUCTURES

The heterojunction phototransistor for optical fiber transmissions has been analyzed by several authors[4–5,7–8]. The dependence of the minimum detectable power on bit-rate has been established as: $P_m \propto \text{bit-rate}$. However, this analysis has to be modified for high current gain-low capacitance

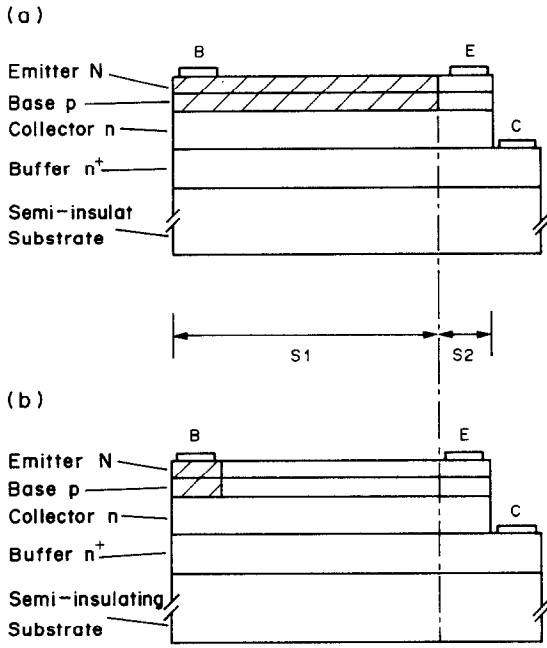


Fig. 1. HPT's technological structures, (a) diffused structure, (b) classical structure.

heterojunction phototransistors for the following reasons:

(i) for a high current gain HPT, the base current is dominated by the recombination current in the base-emitter space charge region I_r , rather than in the base quasi-neutral region I_b . Consequently, in low and medium bias condition where I_r is a dominant current, the current gain varies with the bias current I_c and the noise of the base current cannot be modelled by pure shot noise or partition noise, but rather by recombination noise.

(ii) several technological structures of HPT can be used for integrated photoreceivers. The most widely used is now the diffused structure[9] which presents the advantage of low capacitance compared to a classical structure (Fig. 1). The sensitivity and noise analysis are different for these two structures and an accurate analysis is needed to compared their sensitivity and to take full advantage of HPT's.

Modelling of HPT with respect to its technological structure

In order to compare the performance of both structures, the phototransistor is divided in two regions, corresponding respectively to the photo-sensitive region and the active region of a diffused HPT. With the assumption of a negligible emitter resistivity, equivalent small-signal circuits can be derived. The base-collector and base-emitter capacitances are described by $C_c = C_{c1} + C_{c2}$ and $C_e = C_d + C_{ej2}$ for the diffused structure and $C_c = C_{c1} + C_{c2}$ and $C_e = C_d + C_{ej}$ for the classical structure where $C_{ej} = C_{ej1} + C_{ej2}$, the subscripts 1 and 2 referring to S1 and S2 (Fig. 1). The noise equivalent

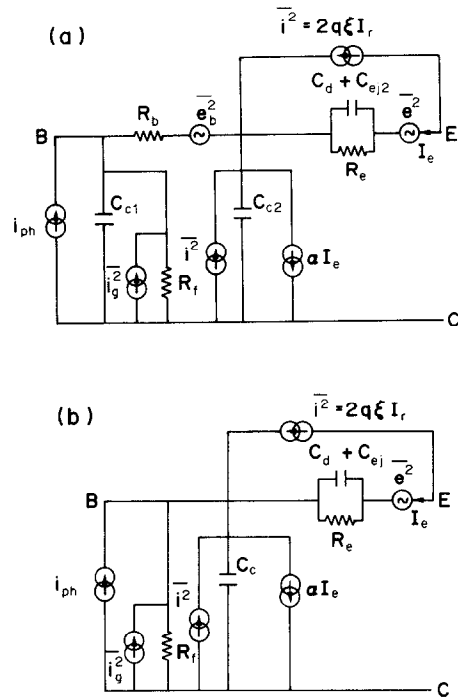


Fig. 2. HPT's noisy equivalent circuit (common collector), (a) diffused structure, (b) classical structure.

circuits can be obtained using the noisy transistor model of Van der Ziel[10] (Fig. 2). As the input current is generated in the base-collector depletion layer, the common-collector configuration is preferred here for obtaining an accurate signal to noise ratio.

The total equivalent noise current density at the input of a diffused HPT is, for $f \ll f_T$;

$$i_{Adif}^2 = 2q[I_b + \xi(\omega)I_r + 2U_T/R_f] + [2R_b C_{c1}^2 + R_e(C_c + C_d + C_{ej2})^2]\omega^2 2U_T q,$$

and for a classical HPT:

$$i_{Acta}^2 = 2q[I_b + \xi(\omega)I_r + 2U_T/R_f] + [R_e(C_c + C_d + C_{ej})^2]\omega^2 2U_T q,$$

where $\xi(\omega)$ is a parameter characteristic of recombination noise, and is a decreasing function of ω with a value between 2/3 and 1/2.

Calculation of the minimum detectable power

Using Personick's notations, the minimum detectable power for a given error rate for HPT is equal to[11]:

$$P_m = \frac{Qh\Omega}{T\eta} [QI_2 + \sqrt{Z}]$$

Q is function of error rate, T is the bit period and $\eta q/h\Omega$ is the responsivity. The noise factor Z can be calculated as:

$$Z = \frac{1}{q^2} \int_{-\infty}^{\infty} [i_A]^2 \left(\frac{H_{out}(f)}{H_{ph}(f)} \right)^2 df,$$

we then obtain:

$$Z_{dif} = \frac{TI_2}{q} \left(I_b + A(T)I_r + \frac{U_T}{R_f} \right) + \frac{(2\pi)^2 I_3 U_T}{Tq} [R_e(C_c + C_d + C_{ej2})^2 + 2R_b C_{c1}^2],$$

$$Z_{cla} = \frac{TI_2}{q} \left(I_b + A(T)I_r + \frac{U_T}{R_f} \right) + \frac{(2\pi)^2 I_3 U_T}{Tq} [R_e(C_c + C_d + C_{ej})^2],$$

where

$$A(T) = \frac{1}{T} \int_{-\infty}^{\infty} \xi(2\pi f) \left(\frac{H_{out}(f)}{H_f(f)} \right)^2 df,$$

and $A(T)$ decreases with bit-rate $1/T$.

In the above calculations, noise sources originating from the second stage are neglected.

Comparison of the two structures

For the same sensitive area and bias current, the difference of the noise factor between the two HPT's structures is:

$$\frac{Z_{dif} - Z_{cla}}{U_T(2\pi)^2 I_3 / Tq} = -2R_e C_{ej1} \times [C_{ej1}/2 + C_{ej2} + C_d + C_c] + 2R_b C_{c1}^2.$$

The diffused structure is more sensitive if:

$$\frac{R_b}{R_e} < \frac{C_{ej1}[C_{ej1}/2 + C_{ej2} + C_d + C_c]}{C_{c1}^2}.$$

For $C_{ej}/C_c > 10$ and $R_e > 25 \Omega$ which are typical values of an HPT, this is verified if $R_b < 1.5 \text{ k}\Omega$ which is almost always true. In a realistic case, the sensitivity of HPT with classical structure is even lower than assumed in this comparison because the emitter series resistance and the effect of emitter current crowding can be very important in a high gain-low capacitance HPT.

This analysis proves that if the base resistance is not too high, the diffused structure is more sensitive than the classical structure even when taking into account in the model of the diffused HPT the noise related to the base access resistance. Since in addition, the dynamic electrical performances of the diffused HPT are higher than those of the classical structure, because of the low input capacitance, this structure has been chosen in our work and only the analysis of this structure will be detailed.

Optimisation of the diffused structure HPT

The optimum bias current I_c depends on the bit-rate and is usually very low as we are going to see now: the base current is dominated by the recombination current in the space charge region I_r , at medium and low bias current for high current gain HPT, and the current gain in this case depends

strongly on bias current:

$$\beta = \frac{I_{cs} \exp(V_{be}/nU_T)}{I_{bs} \exp(V_{be}/mU_T)} \propto I_c^{1-n/m},$$

where m is close to 2 and n is close to 1.

As R_b is independent on bias current for low base current, the optimum bias current I_c can be obtained from $dZ/dI_c = 0$ for a given bit-rate. As $\xi(\omega)$ decrease slowly at high frequency, $A(T)$ can be approximated by a constant in this calculation. The optimum bias current I_{copt} varies as:

$$I_{copt} \propto (\text{bit-rate})^{2/(1+n/m)} \simeq (\text{bit-rate})^{1.33}.$$

At 1 Gbit/s, for $C_c + C_{ej} + C_d = 0.5 \text{ pF}$ and $\beta = 1000$ when $I_c = 5 \text{ mA}$, I_{copt} is around 1 mA.

The minimum detectable power, when thermal noise of the base resistance is low, varies as:

$$Pm \propto (\text{bit-rate})^{(m+3n)/(m+n)/2} \simeq (\text{bit-rate})^{0.83},$$

and $Pm \propto (\text{bit-rate})^{1+n/m} \simeq (\text{bit-rate})^{3/2}$ if the base thermal noise is dominant.

Discussion

The comparison of PIN-FET and HPT has been done by Brain and Smith[5], showing the expected interesting range for HPT was above 1 Gbit/s. With the low capacitance obtained by this structure, HPT's have a high sensitivity even at lower bit-rate (about a few hundreds Mega bits/s) (Fig. 3). Reduction of parasitic noises obtained by integrating HPT with HBT's could lead to an extension of interesting application range.

The error introduced by considering the recombination noise as shot noise or partition noise can be evaluated using the approximation of $A(T)$ by $I_2 \xi(\omega)$, resulting in an increase of total noise factor Z for at least $0.25 TI_2 I_r / q$. Finally, let us conclude with the fact that monolithic receivers with a diffused type HPT are very promising for medium range data

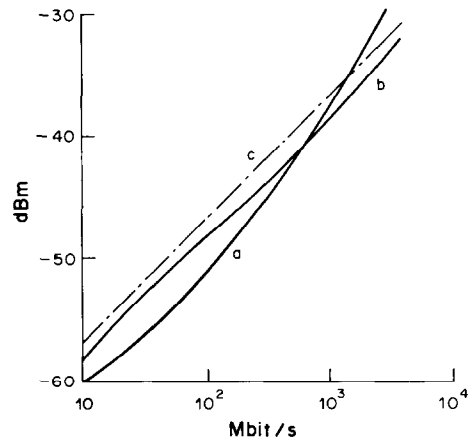


Fig. 3. Comparison of PINFET with HPT, (a) PINFET (from Ref.[5]), (b) high current gain diffused HPT ($\beta = 500$, $R_f = 300 \text{ k}\Omega$, diameter of the photosensitive area = $60 \mu\text{m}$, $C_t = 0.22 \text{ pF}$), (c) classical HPT (from Ref.[5], $\beta = 100$, $C_t = C_d + C_{ej} + C_c = 0.4 \text{ pF}$).

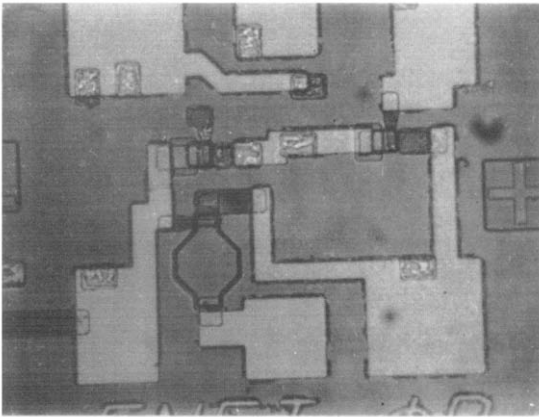
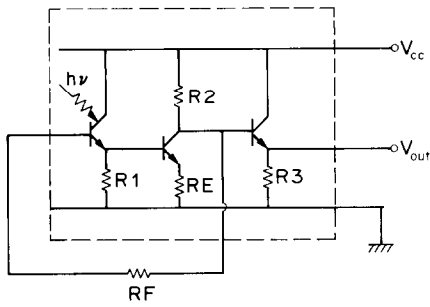


Fig. 4. Circuit diagram and microphotograph of the monolithic photoreceiver. The feedback resistor was not integrated on chip at this stage.

bit rates (a few hundreds Mbit/s) and above, in terms of sensitivity.

3. DESIGN AND EXPERIMENTAL RESULTS OF A MONOLITHIC PHOTORECEIVER

The first monolithic photoreceivers using GaAlAs/GaAs HPT have been fabricated from MBE layers. The chip's dimensions are $0.5 \times 0.5 \text{ mm}^2$ [12] (Fig. 4). The photodetector-preamplifier implementing a HPT, two HBT's and four resistors has been designed with $4 \mu\text{m}$ design rules. The transimpedance configuration was preferred because of its advantages over the high input impedance design in

terms of high stability and large dynamic range. The stability and low sensitivity on the variations of the resistors and other parameters related to HPT and HBT's are ensured by the serie feedback resistor RE. The photosensitive area of the HPT has an equivalent diameter of $56 \mu\text{m}$, compatible with the dimension of multimode fibers. The noise parameter Z for I_c close to the optimum value is predominated by the thermal noise of R_f and R_b . As a result, we have chosen a I_c value larger than optimum to provide a larger bandwidth.

The multilayer structure was grown by MBE with a graded emitter-base interface. The Zn diffusion with Si_3N_4 as mask was performed in order to convert the emitter part of the HPT to p -type (diffused structure), and to reach the base layer for base contact. Boron and proton implantations are used for isolation. The integrated resistors are implanted in the buffer layer, and the SiO_2 is deposited by UVCVD for an antireflecting coat and to passivate the surface (Fig. 5).

The photoreceiver with a $26 \text{ k}\Omega$ external feedback resistor operates from a single 7 V supply voltage. The transimpedance gain has been measured as 7 kV/A , and the noise measurements with a low-pass filter of 70 MHz have shown a noise equivalent power (NEP) of -61 dBm at the output. The measured NEP does not depend on the incident optical power as long as it is in the μW range. Pulse measurement using a GaAs laser operating at $0.82 \mu\text{m}$ and emitting optical pulses of about 100 ps duration has been performed. The exponential falling edge has a time constant of 2 ns which corresponds to a first order pole of the transfer function of 80 MHz (Fig. 6). The discrete Fourier transform computation of the pulse response exhibits a 6 dB roll off and a bandwidth larger than 80 MHz (about 100 MHz). Optical measurement with a $0.85 \mu\text{m}$ LED has shown an electro-optical gain of 1500 V/W . From these experimental results on signal and noise power, one can infer the variations of the signal to noise ratio with optical power. These variations, together with the bandwidth of the receiver (80 MHz) leads to an estimated sensitivity for the receiver of -30 dBm at 140 Mbit/s transmission rate for an error rate of 10^{-9} [13].

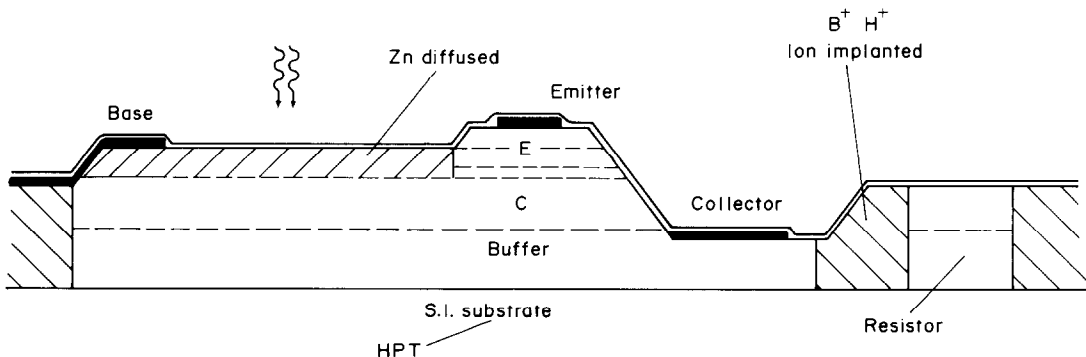


Fig. 5. Cross section of the HPT and resistors implemented in the monolithic photoreceiver. HBT's have the same structure as HPT but without the photosensitive area.

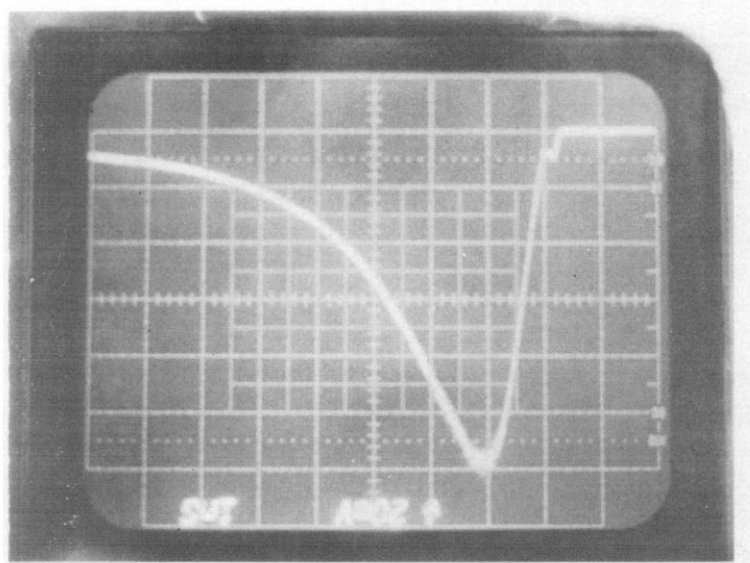


Fig. 6. Response of the monolithic photoreceiver to a short $0.32 \mu\text{m}$ wavelength optical pulse.

HPT characterization: the $I_c(V_{be})$ and $I_b(V_{be})$ plots of HPT and HBT show a diode ideality factor of 1.1 for collector current and 2 for base current which confirm that the base current is actually dominated by recombination current in the space charge region. The noise of the monolithic photoreceiver as analyzed with a spectrum analyzer shows that the noise spectral density decreases rapidly within the bandwidth (Fig. 7). The theoretical noise expression as analyzed previously for this photoreceiver is predominated by the base current noise contribution ($I_b = 27.5 \mu\text{A}$), the comparison of the theoretical and measured results shows that there is an excess “ $1/f$ ” flicker noise which is attributed to the diffusion process and appears in a random way depending on SiN deposition.

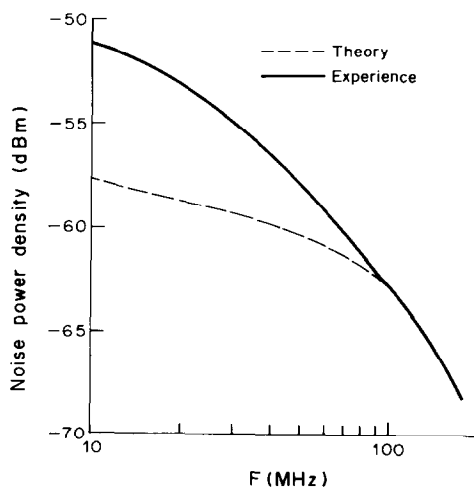


Fig. 7. Noise spectrum of the photoreceiver (amplified by a 23 dB wide-band amplifier). Noise filter: 1 MHz.

HPT's and HBT's in the test zone located in the same area of the wafer than the photoreceiver have been tested. The external responsivity of the HPT has been found to be 93.5 A/W , the responsivity of the base-collector photodiode has been estimated to 0.23 A/W . S-parameter measurements have shown a transition frequency larger than 8 GHz for HBT's and close to 2 GHz for HPT's.

These experimental results exhibit a significant difference with expected electrical performance obtained from the computer simulation. In order to understand this difference, a complete electrical characterization of HBT and HPT has been carried out. An electrical equivalent circuit has been established from S-parameter measurements. It appears that if very low junction capacitances are effectively obtained, relatively high series resistances are observed for the emitter ($R_{ee} = 35 \Omega$) and collector ($R_{cc} = 40 \Omega$). The contact resistance seems to be the origin of these high resistance values. TLM measurements on test structures confirm this prediction. It appears that the Early effect cannot be neglected for establishing the equivalent circuit. From the experimental results obtained on photoreceivers, a very important Early effect is observed in high current gain HPT, because the high current gain requires high base transfer factor which means a thin base layer. The Early effect reduces the output impedance and has a very important role in electrical performance. It does not contribute to a noise generator, but the noise factor can be slightly influenced because the available power gain can become smaller than expected and the noise of the following amplification stage can become significant.

The simulations of the total circuit have resulted in a gain-bandwidth product of $3 \times 10^6 \text{ V/A MHz}$ [14].

The difference with the present $5 \times 6 \cdot 10^5$ V/A MHz is mainly due to the Early effect, the use of non-optimum multilayer structure which increase the collector capacitance, and the high contact resistances. The ultimate sensitivity of this photoreceiver, fabricated with low contact resistances and with optimum multilayer structure (higher quantum efficiency, lower collector capacitance), is expected to be close to -40 dBm for a bit rate of 140 Mbit/s and a bit-error rate of 10^{-9} . This value accounts for a 1.4 dB degradation resulting from the 26 k Ω feedback resistor.

4. CONCLUSION

We have presented the design, fabrication and test results of the first monolithic photoreceiver based on GaAlAs/GaAs HBT technology. The heterojunction phototransistor using a diffused structure is expected to give a high sensitivity at high and moderate bit-rates optical transmissions. For high current gain HPT's, the thermal noise of the base access resistance, the Early effect and the variation of the current gain with bias condition have to be taken into account. The experimental results show that taking advantage of the compatibility between HBT and HPT, a monolithic photoreceiver with heterojunction bipolar devices can achieve high reliability and low parasitic noise. Although the performance obtained is

already one of the best results reported on monolithic photoreceivers at $0.85 \mu\text{m}$, further improvements on available technology should lead to a higher sensitivity (-40 dBm for 140 Mbit/s and 10^{-9} bit-error rate expected) and higher gain-bandwidth product, making this receiver attractive for local area networks.

Acknowledgements—The authors wish to thank A. Scavennec and C. Chevallier for their help in this work.

REFERENCES

1. S. Miura *et al.*, *IEEE Electron Dev. Lett.* **EDL-4**, 375 (1983).
2. R. M. Kolbas *et al.*, *Appl. Phys. Lett.* **43**, 821 (1983).
3. O. Wada *et al.*, *Electron Lett.* **19**, 1031 (1983).
4. K. Tabatabaie-Alavi and C. G. Fonstad, *IEEE J. Quantum Electron.* **QE 1712**, 2259 (1981).
5. M. C. Brain and D. R. Smith, *IEEE Trans. Electron. Dev.* **ED30**, 390 (1983).
6. G. E. Stillman, V. M. Robbins, N. Tabatabaie, *IEEE Trans. Electron. Dev.* **ED31**, 1643 (1984).
7. R. A. Milano *et al.*, *IEEE Trans. Electron. Dev.* **ED29**, 266 (1982).
8. C. Brain and R. Smith, *Electron. Lett.* **18**, 772 (1982).
9. A. Scavennec *et al.*, *Electron Lett.* **19**, 394 (1983).
10. Van der Ziel, *Adv. Electron.* **46**, 313 (1978).
11. S. D. Personick, *Bell Syst. tech. J.* **52**, 843 (1973).
12. H. Wang and D. Ankri, *Electron Lett.* **22**, 391 (1986).
13. P. Le Men *et al.*, *Proc. ECOC* (1978).
14. H. Wang *et al.*, *Proc. ESSCRIC* (1984).